5

Paim, P. S. G., E. L. C. Lavina, U. F. Faccini, A. S. da Silveira, H. Leanza, and R. S. F. d'Avila, 2011, Fluvial-derived turbidites in the Los Molles Formation (Jurassic of the Neuquén Basin): Initiation, transport, and deposition, *in* R. M. Slatt and C. Zavala, eds., Sediment transfer from shelf to deep water—Revisiting the delivery system: AAPG Studies in Geology 61, p. 95–116.

Fluvial-derived Turbidites in the Los Molles Formation (Jurassic of the Neuquén Basin): Initiation, Transport, and Deposition

Paulo Sergio Gomes Paim, Ernesto Luiz Correa Lavina, and Ubiratan Ferrucio Faccini

Universidade do Vale do Rio dos Sinos (UNISINOS)-Programa de Pós-Graduação em Geologia (Brazil), São Leopoldo, Brazil

Ariane Santos da Silveira

Universidade do Vale do Rio dos Sinos (UNISINOS), São Leopoldo, Brazil

Héctor Leanza

Servicio Geológico Minero Argentino-Consejo Nacional de Investigaciones Científicas y Técnicas (SEGEMAR-CONICET) and Universidad Nacional de La Plata, Argentina

Roberto Salvador Francisco d'Avila

Petróleo Brasileiro S. A. (Petrobras), Rio de Janeiro, Brazil

ABSTRACT

This chapter is about an almost uninterrupted exposure of the Jurassic Los Molles Formation in the Arroyo La Jardinera region in the southern Neuquén Basin (western Argentina). It is based on the analysis of high-resolution satellite images linked with extensive field data. Its main goal is to present a conceptual model for the studied turbidite system capable of explaining how sand and gravel were brought onto and removed from the shelf margin and how these coarse-grained sediments were transported along and deposited on the slope and basin plain. The facies tract ascribed to this turbidite system represents high-frequency lowstand system tracts. From proximal to distal, it includes the record of fluvial channels incised into mid- to outer-shelf deposits, turbidite channels scoured on slope strata, turbidite lobes resting on slope rise facies, and poorly developed turbidite lobe fringes enclosed within basin-plain strata. These

DOI:10.1306/13271352St613437

gravity flow strata were assigned to short-lived (surges) moderately efficient turbidity currents derived from the almost continuous failure of delta-front deposits (sand and gravel) during ordinary fluvial floods.

INTRODUCTION

Based on the interpretation of high-resolution satellite images and extensive fieldwork, Paim et al. (2008) connected the gravity flow strata exposed in the Arroyo La Jardinera area (southern Neuquén Basin, Argentina) to submarine ramps (''sensu''; Heller and Dickinson, 1985), including multiple point sources and no major conduit or canyon, related to high-frequency lowstand (shelf-margin) deltas. Similarly, Mutti et al. (2003) had ascribed the succession exposed in the area to turbidite systems closely related to lowstand deltas (their type-A mixed systems). The main difference between both ideas is the ultimate depositional setting of the turbidite strata, whether a slope-to-basinal setting (Paim et al., 2008) or a distal delta-front–prodelta context (Mutti el al., 2003). A regional description of the Jurassic turbidites in the Neuquén Basin is presented by Burguess et al. (2000), but unfortunately the Arroyo La Jardinera area is only briefly mentioned.

Paim et al. (2008) associated the gravity flow deposits of the area with three independent systems: the first type of gravity flow system (GF1) was ascribed to gravel- and sand-rich density flows. Its facies tract encompasses fluvial channels incised into mid- to outer-shelf deposits, turbidite channels scoured on slope strata, turbidite lobes resting on slope rise facies, and poorly developed lobe fringe facies enclosed within the basin-plain strata. The second type corresponds to a sand-rich system with abundant stratification, including an oscillatory component, which was ascribed to low-concentration combined density flows (GF2). The third system is related to mass gravity flows (slumps and slides) and derived debris flows (GF3). A full description of the entire set of gravity flow deposits and enclosing facies within the Los Molles Formation exposed in the Arroyo La Jardinera area can be found in Paim et al. (2008).

This chapter focuses on the previously mentioned type-1 gravity flow system (GF1), by far the most important in terms of sand and gravel deposition in the study area. It presents many features that reveal several important issues related to the removal of coarse-grained sediments from the shelf margin (triggering processes) and their subsequent transport to the deep sea through sediment gravity flows. In terms of gravity flow initiation, some pieces of evidence suggest that type-1 gravity flows derive from long-lived hyperpycnal currents, whereas other data evoke short-lived depletive surges. In addition, some features indicate that fluid turbulence and other supporting mechanisms are major, but diverse, factors on suspended-load transport. Last but not least, some data indicate a strong connection of the GF1 deposits with high-frequency accommodation cycles and paleophysiography.

Therefore, our main goal is to discuss and present a conceptual model for the GF1 system capable of explaining how sand and gravel were brought into and removed from the shelf margin and how these coarse-grained sediments were transported along and deposited on the slope and basin plain.

GEOLOGICAL SETTING

The Neuquén Basin, located in central western Argentina and eastern Chile, extends northward along the axis of the Andean Cordillera up to 31°S. Between 34°S and 37°S, the basin is restricted by the cordilleran belt as a narrow north-south elongated strip, whereas southward, it broadens eastward into the extra-Andean domain, where it is known as the Neuquén Embayment. The Neuquén Basin features a triangular shape, covers more than 160,000 km^2 (61,700 mi^2), and extends up to 700 km (434 mi) in a north–south direction (Zavala, 1993). Besides the Andean chain to the west, this basin is bounded by the Pampeano-Sierra Pintada and North Patagonian massifs (Figure 1). The infill of the Neuquén Basin (Figure 2) ranges from late Triassic to Paleocene in age (Ramos, 1998) and exceeds 7000 m (22,900 ft) of marine and continental strata (epiclastics, carbonates, evaporites, and pyroclastics).

During the late Triassic, central western Argentina and eastern Chile underwent extensional stresses related to an arc/trench system developed along the western margin of the South American plate (Legarreta and Uliana, 1991; Gulisano and Gutierrez Pleimling, 1995). At that time, sedimentation was confined to isolated fault-bounded depressions controlled by structural features of the underlying sialic substrate. These depressions were filled with nonmarine facies, strongly influenced by pyroclastic and volcanic rocks, presenting abrupt thickness changes (Gulisano and Gutierrez Pleimling, 1995) and known as the Precuyo Group

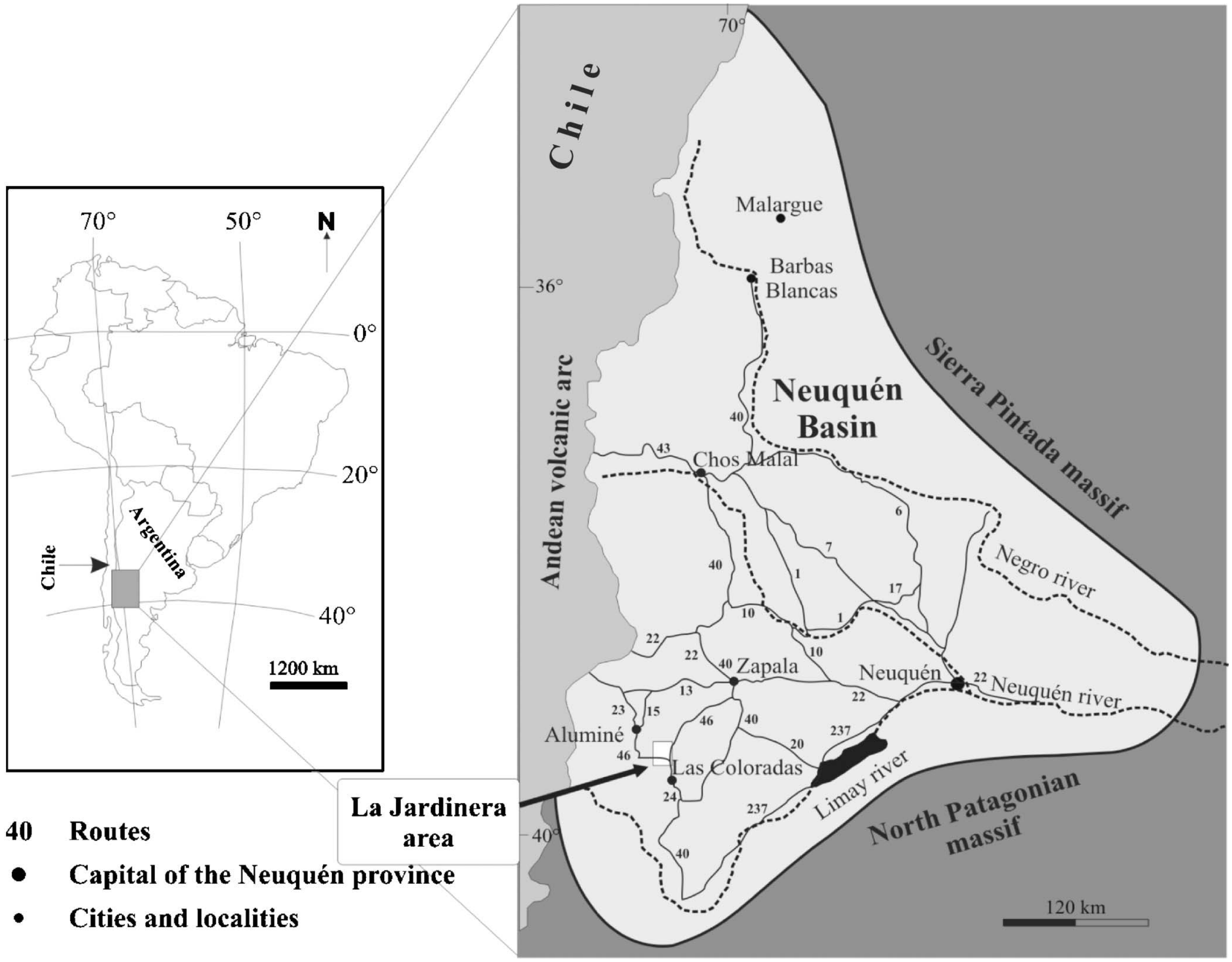

FIGURE 1. The Neuquén Embayment in South America and the location of the study area (Arroyo La Jardinera).

(Lapa Formation in southern Neuquén). These depocenters, sited on the east of the arc/trench system, became ever more unified to ultimately (Pliensbachian) merge into an extensive area of marine sedimentation placed between the volcanic arc to the west and the South American foreland to the east (Vicente, 2005).

From the early Jurassic to part of the middle Jurassic, deposition was chiefly driven by tectonics, a phenomenon that steadily reduced, giving way to a regional subsidence stage from the middle Jurassic to the early Paleogene (Ramos, 1998). Although most of the Neuquén Basin has maintained a nearly steady subsidence rate, records of local episodes of uplift, folding, erosion, and synsedimentary tectonics (Vergani, 2005) exist. Accordingly, sedimentation style and stratigraphic succession are records of those episodes of structural inversion and allied unconformities. The most important of such events produced the Huincul arch, a large east–west transcurrent fault zone in the southern Neuquén Basin associated with extensional stresses caused by the Gondwana fragmentation and ensuing Atlantic Ocean opening (Vergani et al., 1995). Several transgressions and regressions, mainly driven by eustatic sea level changes, occurred before the progressive growth of the Andean chain and cut off any oceanic influence into the basin (Legarreta and Gulisano, 1989). A rise in Andean tectonic activity as from the Miocene made the basin evolution even more complex.

The database used herein comes from the analysis of seismic-scale ($10 \times 10 \times 1.6$ km [$6.2 \times 6.2 \times 0.99$ mi]) high-resolution satellite images and the examination and logging (sedimentologic and gamma ray) of large natural exposures and road cuts. Bedsets and key stratigraphic surfaces can be followed for distances more than 10 km (6.2 mi). The adopted sequence-stratigraphic approach is similar to the approaches proposed by Van Wagoner et al. (1988, 1990), as sequence

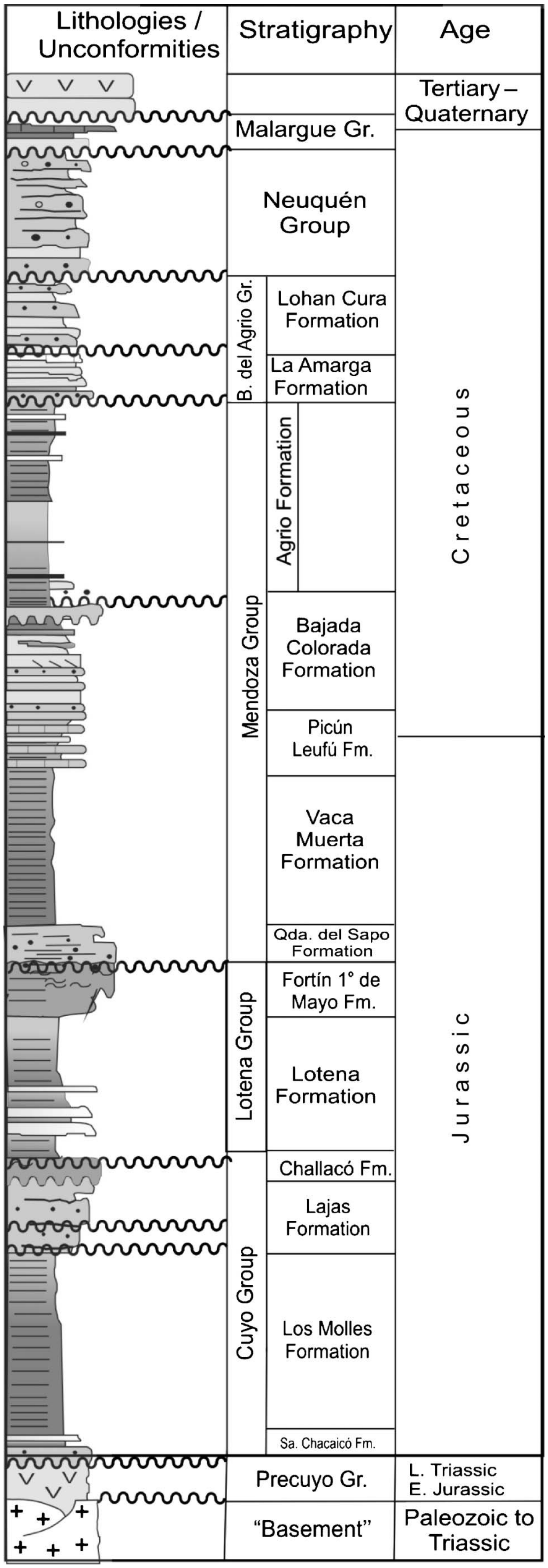

FIGURE 2. **Regional stratigraphic column for the southern and central parts of the Neuquén Basin (modified after Leanza and Hugo, 1997). The studied interval comprises part of the Los Molles and Lajas formations. Gr. = Group; B. = Bajada; Fm. = Formation; Qda. = Quebrada; Sa. = Sierra, L. = Late; E. = Early.**

boundaries are tied to the end of base-level fall, and by Hunt and Tucker (1992) and Helland-Hansen and Gjelberg (1994), as four system tracts are discriminated (lowstand, transgressive, highstand, and falling stage).

In the study area, a main unconformity (sequence boundary 1 [SB1]) outlines the base of the Cuyo Group and corresponds to the boundary between the Los Molles and Sierra Chacaico formations (Figure 3). The Cuyo Group comprises 1100 m (3600 ft) of deep-marine strata (Los Molles Formation), 550 m (1800 ft) of shelfal to coastal facies of the Lajas Formation (between SB5 and SB8) and, at the top, the red beds of the Challacó Formation (Figure 4). The studied section is bounded by SB2 and SB6 and includes the middle and upper parts of the Los Molles Formation as well as its transition to the Lajas Formation (Figures 3, 4). It was subdivided into four 3d-order depositional sequences (J21–J24) that encompass nearly 6 m.y. (Figure 4).

In the ensuing sections, the database is presented to highlight the main themes used to understand the turbidity currents in terms of initiation, transport, and deposition, and therefore to support the conceptual model proposed to explain the GF1 system.

MAIN FEATURES

Physiography

Based on the analysis of the facies, facies associations, and architectural elements, the Los Molles and Lajas formations have been ascribed to four paleophysiographic elements, that is, genetic units larger than architectural elements and analogous to present-day physiographic units from several marine basins (Paim et al., 2008). They include the slope rise or basin plain and the slope in the Los Molles Formation, the mid or outer shelf, including the shelf margin, at the transition between the Los Molles and the Lajas formations, and the inner shelf or nearshore in the Lajas Formation (Figures 3, 4). These 10- to 100-m (33- to 330-ft)-thick paleophysiographic units include smaller, few to several meters thick, architectural elements with distinct geometries and facies associations (Figure 4).

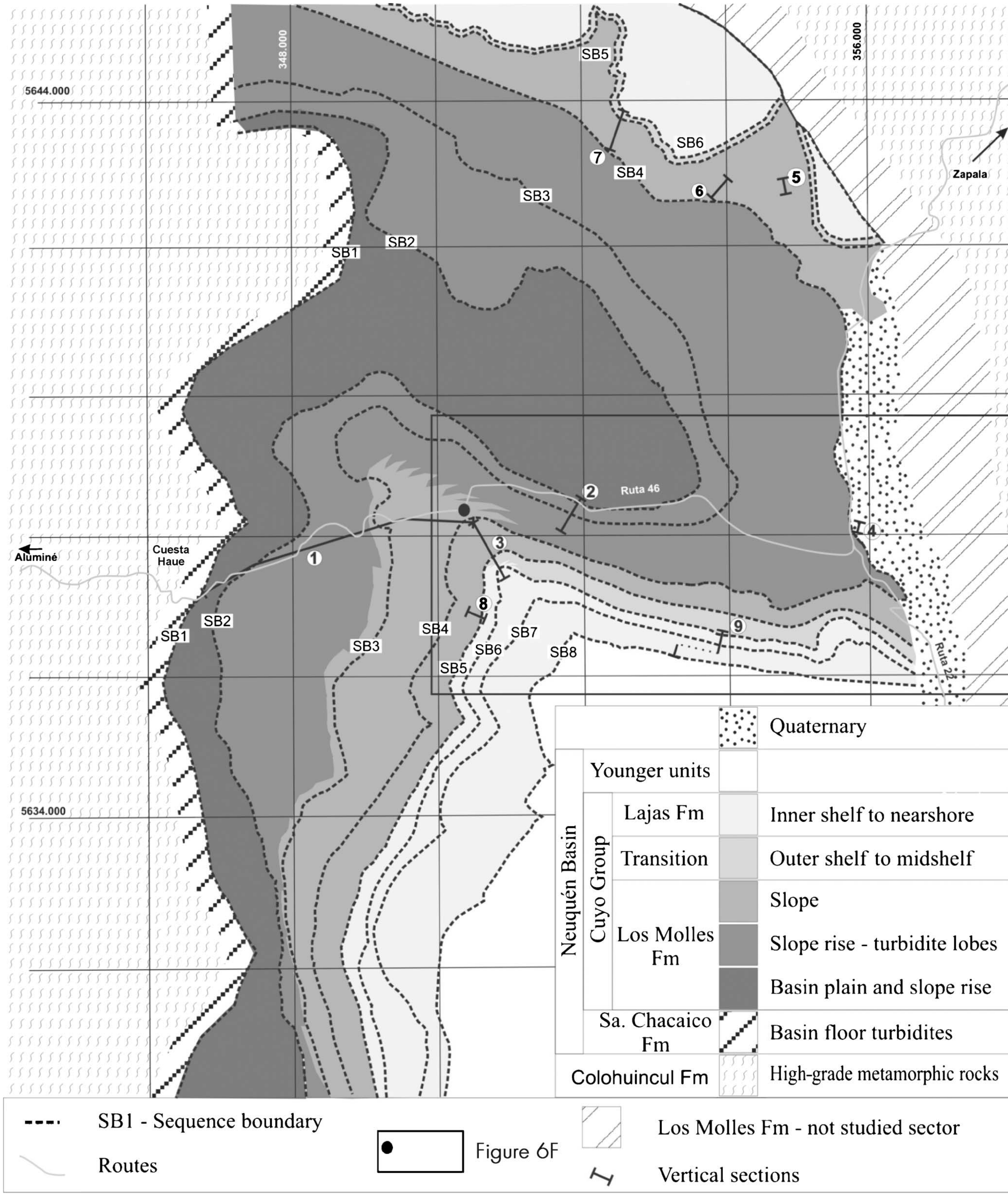

FIGURE 3. Geological units in the study area (Arroyo La Jardinera Region) and paleophysiographic elements and sequence boundaries in the Los Molles and Lajas formations from the interpretation of a high-resolution satellite image (by IKONOS). The acquisition scale of the vertical sections ranges between 1:100 and 1:500. Fm = Formation; Sa. = Sierra.

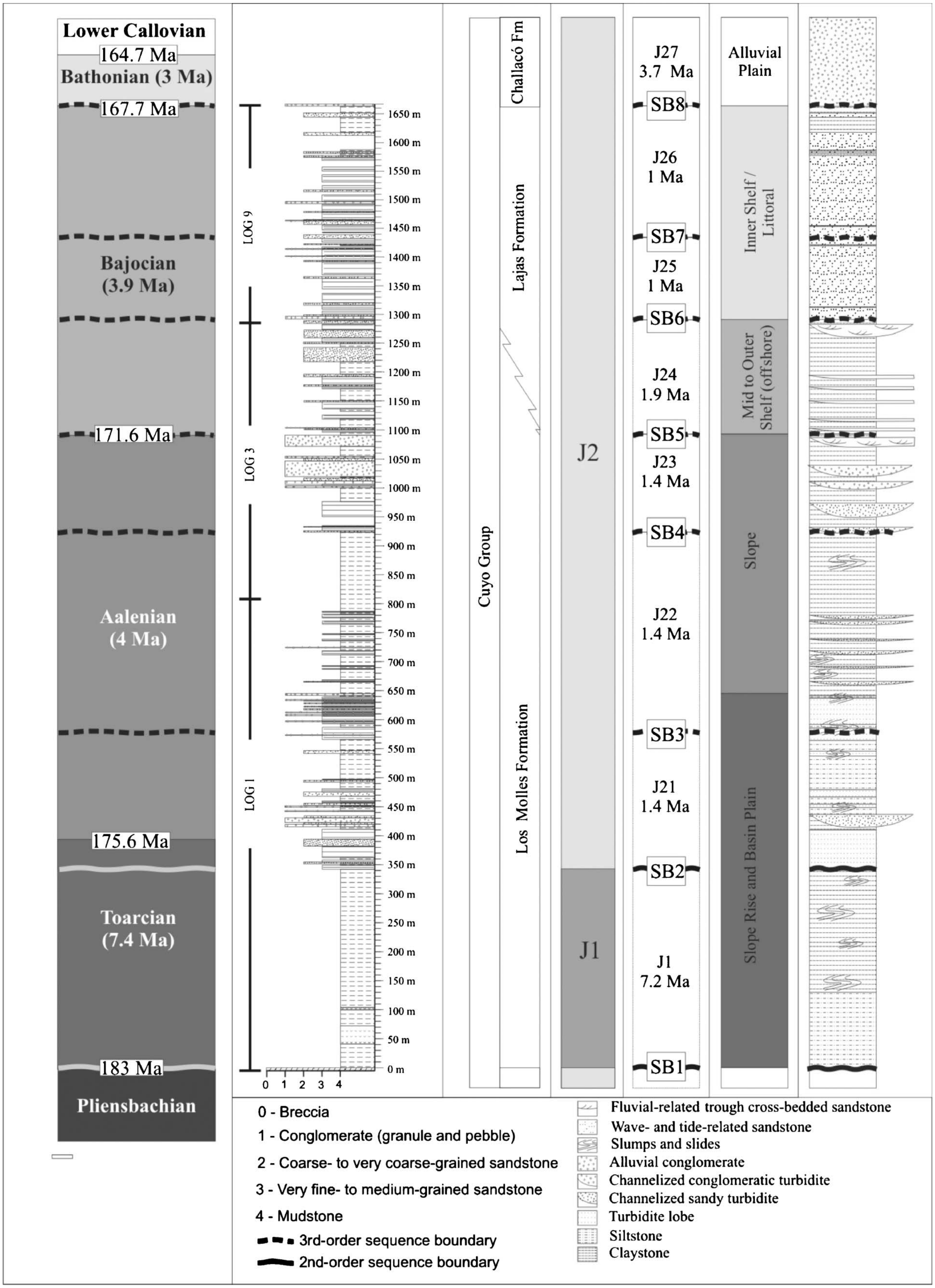

FIGURE 4. Simplified composite vertical section of the study area. Stages obtained from correlation to Gulisano and Gutierrez Pleimling (1995) chart and absolute ages from Gradstein et al. (2004) chart. SB = sequence boundary; Fm = Formation; J21– J27 = 3rd-order depositional sequences; J1, J2 = 2nd-order depositional sequences.

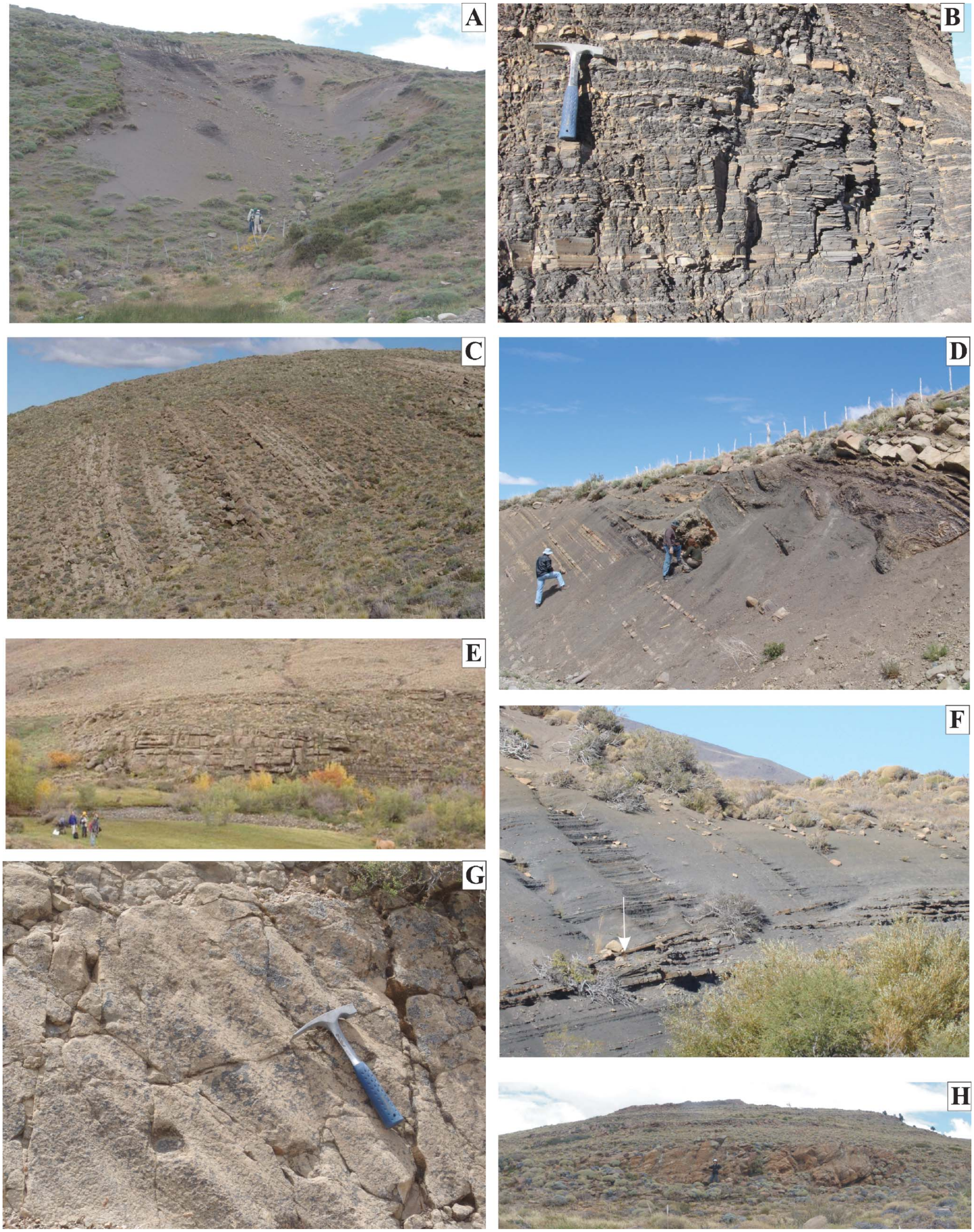

FIGURE 5. Physiography: (A) Fine-grained and (B) heterolithic lobe fringe deposits related to basin plain; (C) lobe sandy (sandstone bedset ranges from 5–15 m [16.4–49.2 ft] in thickness) and (D) slumped beds ascribed to the slope rise; (E) turbidite channel and (F) slide (white arrow) associated with slope strata; and (G) falling-stage wave-rippled sandstone resting on outer-shelf mudstone and scoured by (H) incised channel-fill facies.

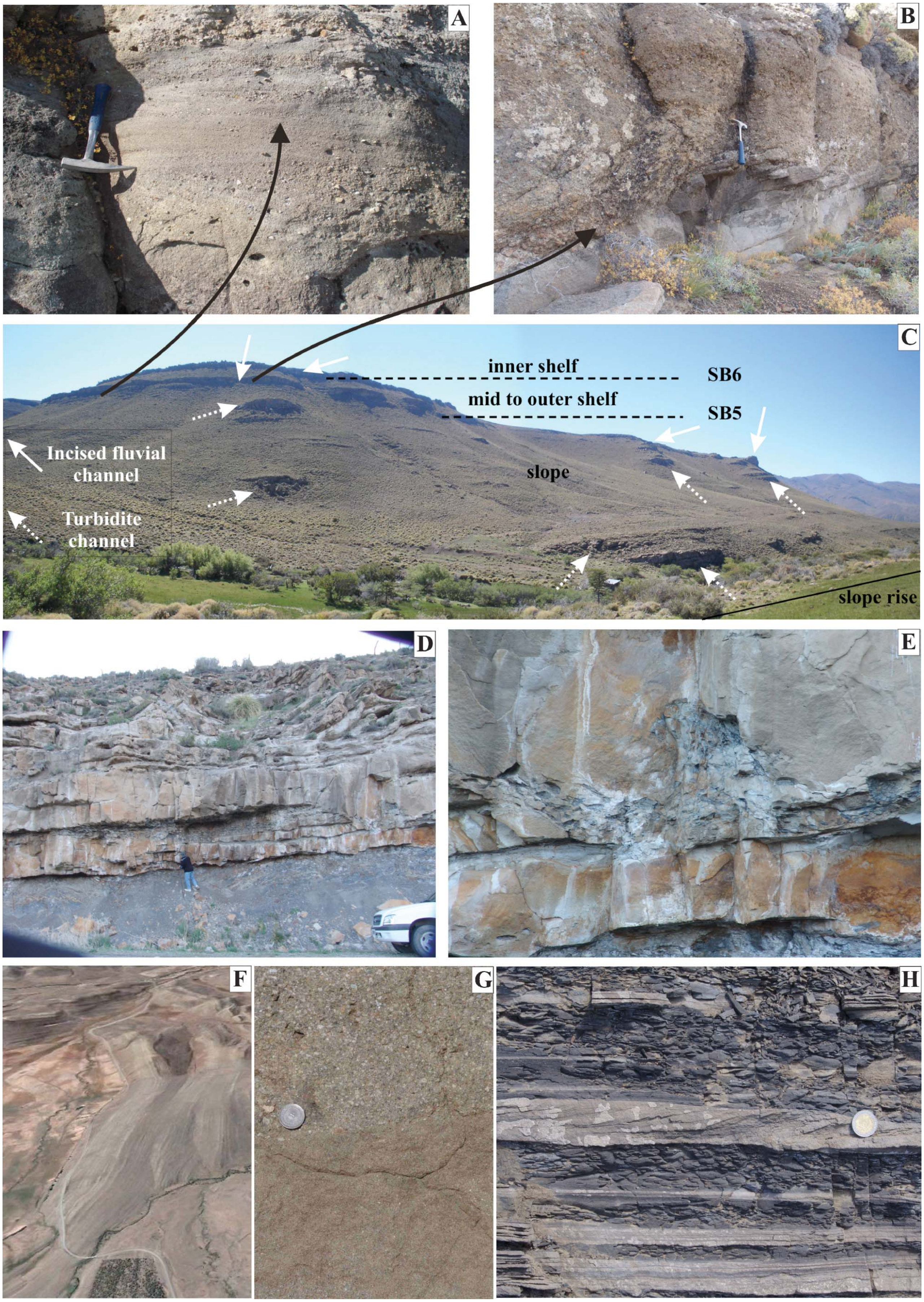
A
B
C
inner shelf
SB6
mid to outer shelf
SB5
Incised fluvial
channel
slope
Turbidite
channel
slope rise
D
E
F
G
H

In the Los Molles Formation, profuse fine-grained deposits (Figure 5A, B), tabular beds of sandstone sets ascribed to turbidite lobes (Figure 5C), fossil-rich (ammonites and small bivalves) layers, and dominantly planktonic radiolarian specimens among the microfauna (Kochhann et al., 2009) characterize the slope rise to basin plain. The distinction between slope rise and basin-plain strata is based on the exclusive occurrence of slumped beds in the former (Figure 5D). Similar faunal content, slumped beds, commonly coupled with slide deposits (Figure 5F), and turbidite channel fills encased by muddy interchannel facies (Figure 5E) define the slope realm. The transition between the Los Molles and Lajas formations consists of mid- to outer-shelf siltstone, sporadically enclosing sharp-based nearshore facies (Figure 5G) scoured by fluvial channels (Figure 5H). Lastly, a sandy interval (Lajas Formation), which includes wave-, storm- and tidal-related structures and some muddy intervals a few meters thick, defines the inner-shelf–nearshore paleophysiographic element.

Basin-plain shale and lobe–lobe fringe turbidites of the lower and mid–Los Molles Formation, respectively, followed by turbidite and incised fluvial channels encased in extensive fine-grained facies of the slope (upper Los Molles Formation) and mid to outer shelf (transition from Los Molles to Lajas formations), in that order, make up a succession that is very similar to that presented by Gulisano and Gutierrez Pleimling (1995) for the same area. This succession is supposed to be an outcrop analog of the tripartite subdivision of the Los Molles Formation defined by Gómez Omil et al. (2002) and Verzi et al. (2005) from seismic data.

In short, the GF1 system is linked to a paleophysiography composed of two gently dipping surfaces (shelf and basin plain) separated from each other by a steeper unstable slope. The thickness of the slope succession (about 400 m [1300 ft] thick; Figure 4) suggests a fairly deep-water setting (hundreds of meters of water depth) for the basin-plain facies. Similar physiography and water depth of the basin-floor turbidites were described by Steel et al. (2000).

Architectural Elements

The basinward tract of architectural elements of the GF1 system encompasses incised fluvial channels (shelf and shelf margin), turbidite channels (slope), and widespread turbidite lobes and lobe fringes (slope rise and basin plain).

The downdip and vertical changes of the GF1 architectural elements (Figures 3, 4) illustrate the basinward transition from incised fluvial channels through turbidite channels to turbidite lobes and lobe fringes (Figure 6). Incised fluvial channels are encased within shelf to shelf-margin strata; turbidite channels are scoured into and surrounded by slope, commonly remobilized fine-grained deposits; and turbidite lobes and lobe fringes are enveloped by fine-grained slope rise and basin-plain facies.

Facies Tract

Plane- and cross-bedded sandstone and both massive and stratified clast-supported conglomerates with sparse wood pieces represent the main fluvial channel-fill facies (Figure 7A–C). A minor tidal influence is suggested by the rare presence of rippled fine-grained sandstone with flaser and mud drapes near the base of the channel fills. Together, these pieces of evidence, in addition to the lack of sedimentary features associated with hyperconcentrated flows (sensu; Pierson and Costa, 1987), point to prevailing usual conditions of fluvial transport and deposition within incised braided fluvial channels, even during flood events (i.e., ordinary floods).

In contrast, the turbidite channel fills display a clear basinward reduction in mean grain size from clast-supported through matrix (sandy)-supported conglomerates to sandstones (Figure 7D–G). This down-dip segregation strongly suggests that fluid turbulence was a major factor in the long-distance transport of gravel and sand. This inference is reinforced by profuse flute casts at the base of the turbidite channels (Figure 8E) and rip-up clasts near their bases (Figures 7G, 8C). However, nonturbulent granular flows are indicated by the massive (Figure 7D–G) nongraded nature of most of the turbidite channel-fill beds. Their simple (in opposition to complex) and relatively thin character (0.1–0.5 m [0.33–1.6 ft]; Figure 8A, C) suggests short-lived currents. Jointly, both sets of data point to turbulent surges that developed downcurrent, with ever finer grained basal granular layers as a result of gravity transformation (sensu; Fisher, 1983).

FIGURE 6. **Architectural elements and facies associations: (A, B) Incised stratified fluvial deposits (see arrows for location); (C) turbidite and fluvial channels scoured on slope and shelf-margin facies, respectively; (D, E) massive turbidite channel strata; (F, G) tabular bedsets of massive sandstone related to the turbidite lobe; and (H) thin-bedded turbidites of the lobe fringe. SB = sequence boundary.**

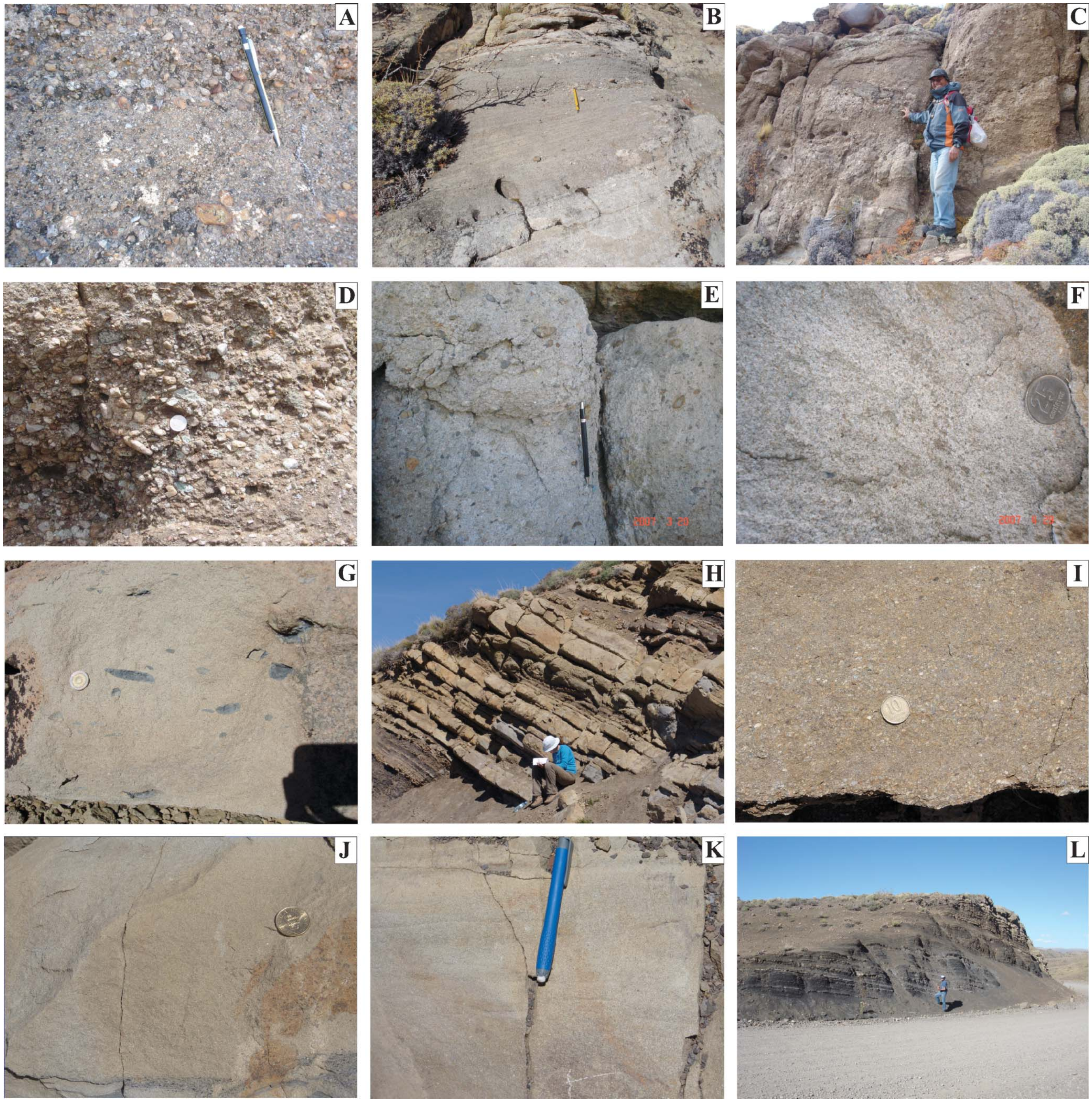

FIGURE 7. **Facies tract: Clast-supported conglomerate (A) and plane and trough cross-bedded sandstone (B), sometimes with large pieces of trunks (C), associated with incised fluvial channel fill; clast (D)- and matrix (E)-supported conglomerate and massive sandstone (F), usually with rip-up clasts (G), related to turbidite channel fill; laterally extensive turbidite lobe strata (H) comprising massive coarse (I)- to fine (J)-grained sandstone, occasionally with incipient lamination (K); and heterolithic deposits (L) of the lobe fringe.**

Downcurrent turbidite lobe and lobe fringe facies display similar features to those of the turbidite channel fills, except for their extensive geometry (Figures 5C, 6F, 7H, 8B), finer grained nature (Figure 7I–K), less abundant flute casts and rip-up clasts (Figure 8D, E), and more frequent normal grading (Figure 8F) and plane bedding (Figures 7K, 8G). Relative to turbidite channel fill, lobe strata are supposed to represent similar bipartite turbidity currents, but moving a finer grained suspended load in poorly constrained to wholly unconfined flows.

In short, GF1 deposits have been related to short-lived bipartite turbidity currents. Fluid turbulence has acted as the main supporting mechanism in

FIGURE 8. **Surgelike density flow suggested by discrete medium-scale sedimentary bodies within turbidite channels (A) and lobes (B); pieces of evidence pointing to the turbulent nature of the long-distance transport, including rip-up clasts in both turbidite channel (C) and lobe strata (D), common to abundant flute casts at the turbidite channel base (E) and normal grading (F) and plane bedding (G) in turbidite lobe strata; and nearby continental sources indicated by common plant debris within both turbidite channel (H) and lobe (I) deposits.**

long-distance transport of the coarse-grained suspended load from the shelf margin to the deep sea. However, the massive nongraded nature of most of the turbidites indicates that nonturbulent flow conditions would have left the ultimate mark on the deposits themselves. This non-Newtonian (pseudoplastic) rheology is supposed to represent transient conditions confined to the basal layer of the bipartite density flows and produced just before deposition could occur through frictional freezing.

Paleocurrents

Paleocurrent readings of trough cross-bedding within fluvial beds (incised channels) point to east–northeastward effluents (mean value, 83°; n = 24). Flute casts on turbidite beds show a similar trend (mean value, 67°; n = 60). All together, GF1 paleocurrent data point to northeastward currents (mean value, 72°; number of readings (n) = 84) that are similar to the inferred sediment transport path proposed for the area by Burguess et al. (2000) This mean value is roughly orthogonal (angle of 87°) to that presented by wave-induced cross-bedding (mean value, 159°; n = 126) ascribed to alongshore currents (Figure 9). It is also worth noticing that the sediment dispersal trends of both GF1 and nearshore systems have not changed with time (Figure 10).

The aforementioned paleocurrent data strengthen the idea of some genetic linkage between fluvial effluents and turbidity currents. Both dispersal systems comprise multiple small-scale source points (Figure 6C),

(A)

Depositional systems	Morphological element - sedimentary structure - mean paleocurrent vector		General mean vector
Nearshore, wave and tidal current.	Upper shoreface (trough cross-bedding - 122 readings - mean vector: 159) Flood tidal delta (trough cross-bedding - 4 readings - mean vector: 154)	159	GF1 n = 84 n = 126
GF1 system tract	Muddy slope rise and plain and lobe fringe (current ripples - 22 readings - mean vector: 63) Turbidite lobe (flutes, current ripples, and rare trough cross-bedding - 9 readings - mean vector: 105) Turbidite channel (flutes and a few trough cross-bedding - 29 readings - mean vector: 59) Incised fluvial channel (trough cross-bedding - 24 readings - mean vector: 83)	72	

(B)

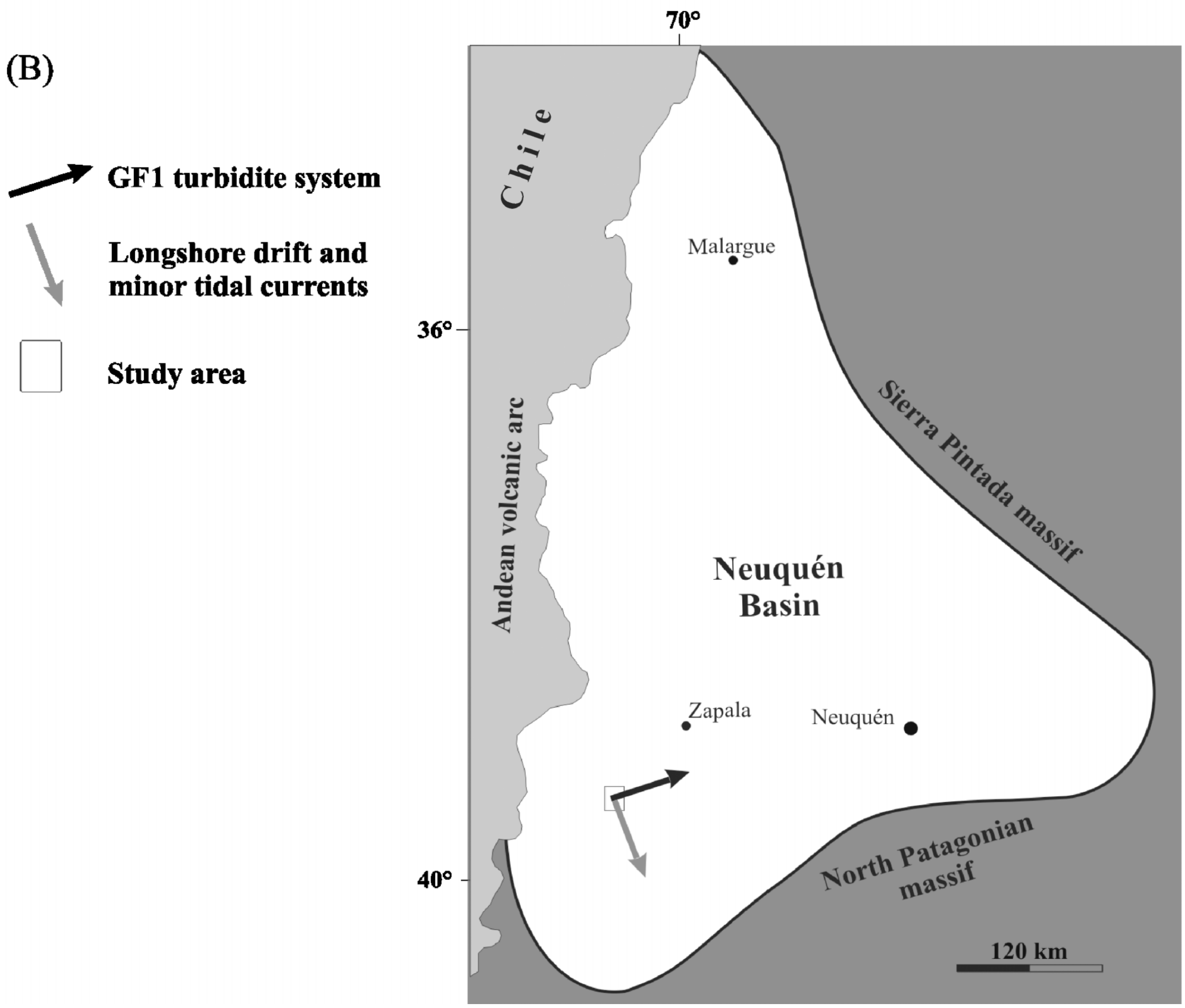

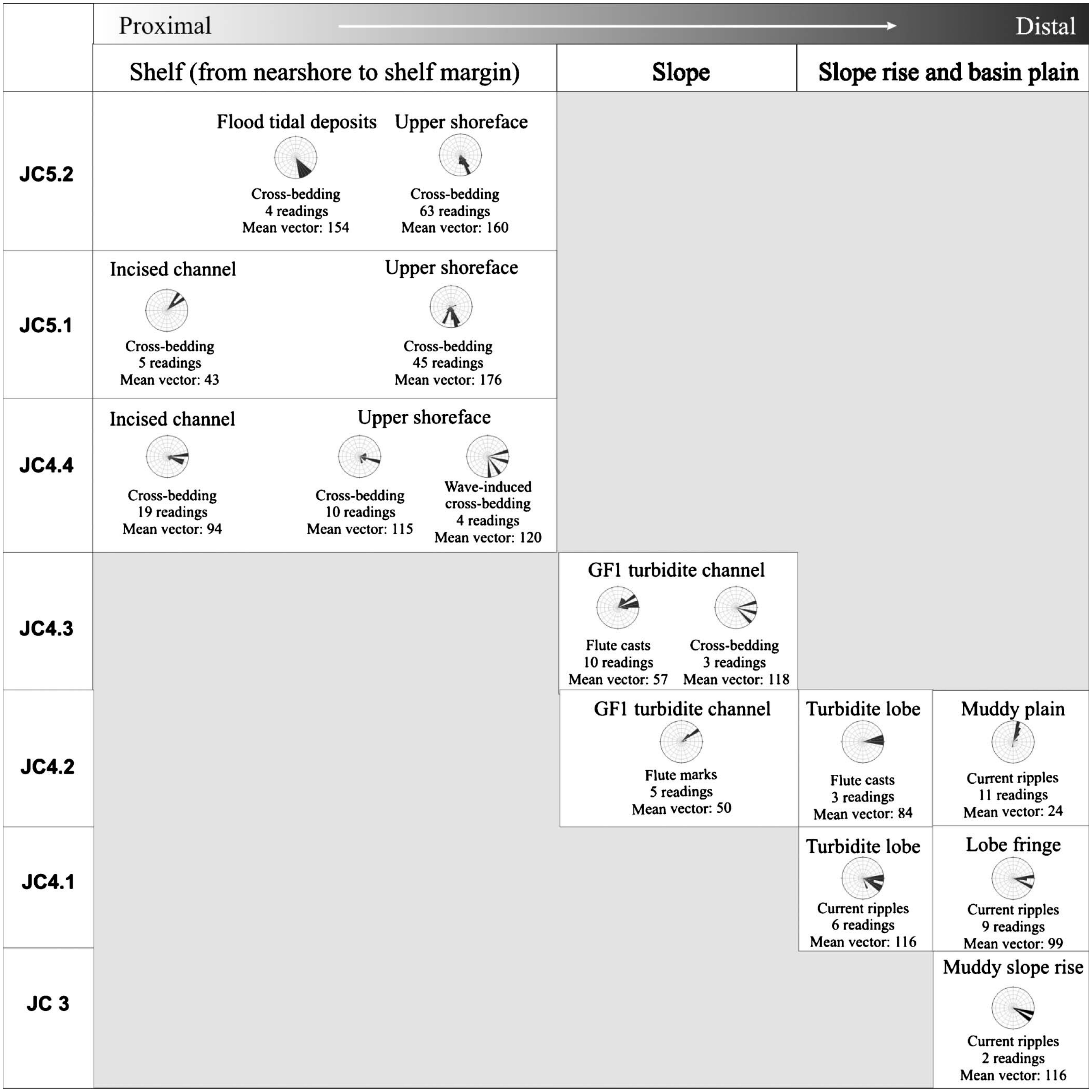

FIGURE 10. Paleocurrents of the first type of gravity flow system (GF1) through time and space. Nearshore, and wave- and tide-induced paleocurrents are also shown for comparison. Notice the steady transport trend of the GF1 strata within distinct paleophysiographic elements, from shelf to basin plain, as well as along time through different 3d-order depositional sequences.

FIGURE 9. The first type of gravity flow system ([GF1] fluvial and turbidity currents) and nearshore, mostly alongshore currents in the study area displaying mean vectors at right angles (A). In the map (B), notice alongshore currents parallel to the presumed local basin margin (north-northwest–south-southeast) and northeasternward toward the basin depocenter GF1 fluvial and turbidity currents. n = number of readings.

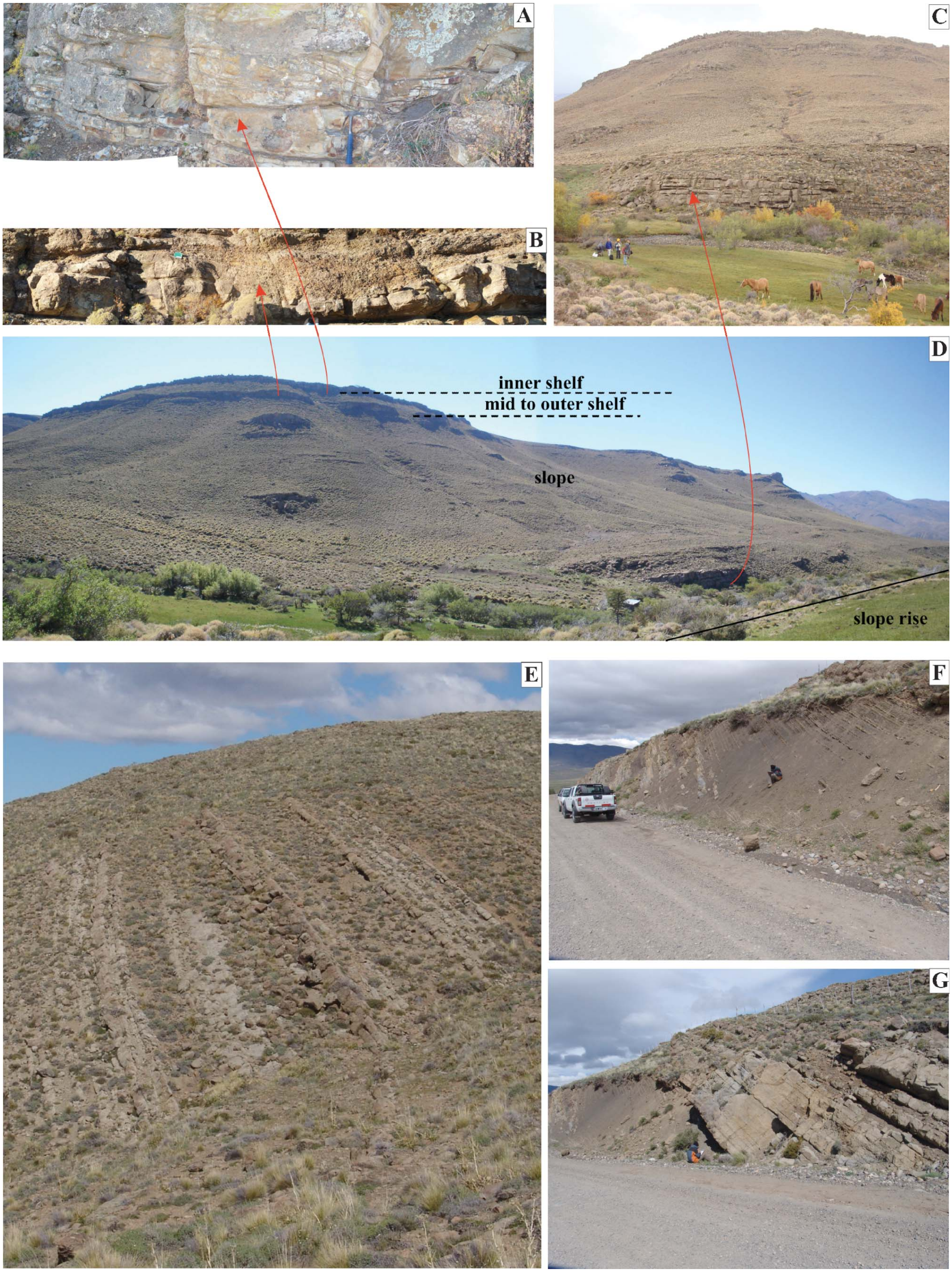
A
B
C
D
inner shelf
mid to outer shelf
slope
slope rise
E
F
G

and they have always flowed toward the basin depocenter, whereas alongshore transport is parallel to the orientation of the local basin border (Figures 9, 10).

High-frequency Sequences

The Cuyo Group is subdivided into two 2d-order depositional sequences, named J1 and J2, which record around 7 and 12 m.y., respectively (Figure 4). A key surface (SB2) delineates their boundary and the onset of a thick package of sandy turbidites that abruptly rests upon a thick package mostly composed of deep marine shale (Figures 3, 4). The J1 depositional sequence comprises the base of the Los Molles Formation, and it records a transgressive-regressive succession. The upper depositional sequence (J2) consists of the Los Molles (mid and upper sections), Lajas, and Challacó formations, and records a regressive unit (Figure 4). The latter sequence is subdivided into seven 3d-order depositional sequences (J21–J27), each one recording 1 to 3 m.y. (Figures 3, 4) and comprising up to two paleophysiographic elements (Figure 3). Besides, the analysis of the facies successions within all paleophysiographic elements and sequences indicates a high-frequency (4th- to 5th-order) modulation of the geological record, which is the theme of the next paragraphs (see also Figures 11, 12). The stacking pattern presented by the turbidite strata exposed in the study area has been used by Mutti (1992) as an example of high-frequency cyclicity on the scale of facies sequences.

In the outer- to midshelf strata, transgressive and highstand mudstones are sharply overlain (regressive surfaces of marine erosion) by wave- and tide-related nearshore deposits of the falling-stage system tract (Figures 5G; 11A, D). In turn, these nearshore facies are then scoured by small fluvial channels (Figure 6B, C) related to the later development of the falling-stage system tract and ensuing expansion of the subaerial unconformity. At the start of relative sea level rise, incised channels were then filled by fluvial (Figures 5H; 6A, B; 7A–C; 11B, D) locally tide-influenced facies. The subsequent increase in the rate of relative sea level rise once more drives the onset of the transgressive system tract over the shelf and consequent extensive silt deposition. In short, high-frequency relative sea level oscillations are recorded in outer- to midshelf strata by the falling-stage (regressive surface of marine erosion and succeeding fluvial incision), lowstand (channel-fill), and transgressive (shelfal siltstone above the surfaces of maximum regression) system tracts.

In the slope, by the end of the falling stage, widespread mudstone connected to the previous system tracts (transgressive, highstand, and falling-stage) was scoured by point-sourced turbidity currents (Figures 6D, E; 11D). Through the lowstand stage, the resultant channels were then filled by amalgamated lenses of gravel- to sand-rich upward and downdip fining turbidites (Figures 6C; 7D–F; 11C). Channel abandonment and resuming widespread mud deposition define the beginning of a new transgressive episode. Thus, 4th- to 5th-order relative sea level fluctuations are recorded in the slope by turbidite scour (early lowstand), turbidite channel fill (late lowstand), and widespread mud deposition (transgressive, highstand, and falling-stage system tracts).

On the slope rise and proximal basin plain, mudstone credited to a preceding high-frequency cycle (late lowstand, transgressive, highstand, and falling-stage system tracts) are regularly overlain (Figure 11G) by tabular bedsets (Figures 5C; 6F; 11E) composed of sand-rich (Figures 6G; 7I–K) few decimeters thick (Figures 7H; 8B) turbidites that supposedly represent the early lowstand system tract. A new increase in the rate of relative sea level rise leads to the deposition of a mud blanket over the sandy turbidites (Figure 11E, F). This package, which is between few to few tens of meters thick, of fine-grained deposits includes the subsequent late lowstand, transgressive, highstand, and falling-stage system tracts.

DISCUSSION

Short- Versus Long-lived Sediment Gravity Flows

Some features suggest a close link between fluvial discharge and sediment gravity flows. The tripartite basin physiography and high-frequency lowstand context promote appropriate conditions for the initiation of turbidity currents from hyperpycnal flows (e.g., Steel et al., 2000; Plink-Björklund and Steel,

FIGURE 11. High-frequency depositional sequences: (A) sharply based tidal bar deposits (falling stage) and (B) incised fluvial strata (lowstand), both within dominantly muddy shelfal strata; (C) sandy turbidite channel (lowstand) surrounded by muddy slope facies (sandstone bedset ranges from 5–15 m [16.4–49.2 ft] in thickness); (D) relative location of (A), (B), and (C); (E) general view of the high-frequency depositional sequences on the slope rise to basin-plain realm (active and abandonment phases of the turbidite lobes); and detailed view of the upper (F) and lower (G) abrupt limits of the lobe bedsets (sandy facies related to the lowstand active phase) with the dominantly muddy deposits (abandonment phases) ascribed to the transgressive and highstand systems tracts.

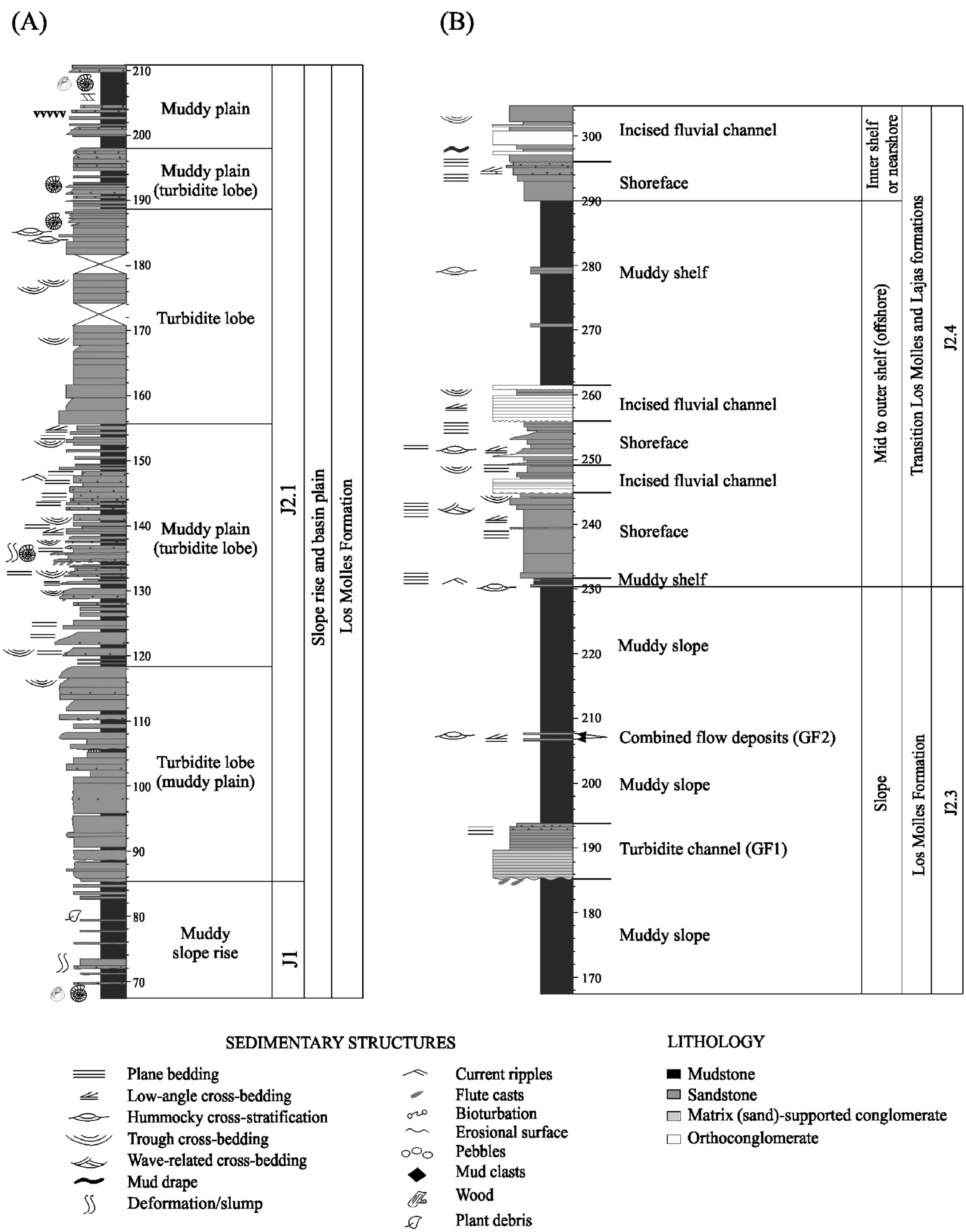

FIGURE 12. Segment of logs 2 (A) and 7 (B). Notice the high-frequency signal modulating the stratigraphic architecture. See log location in Figure 3. Log depths in m. J1 = 2d depositional sequence; J2.1–J2.4 = 3d order depositional sequences.

2004). It is worth noticing that the GF1 facies tract records a downdip change from fluvial facies through gravel- to sand-rich sediment gravity flows. In addition, the fluvial and GF1 systems show parallel paleocurrent trends, a wide range of available grain size (gravel to very fine-grained sand) and prolific plant debris (Figure 8H, I). These data reveal some sort of connection between the fluvial effluents, which delivered sand and gravel to the shelf margin and the GF1 system. However, no support exists in the fluvial deposits to indicate high-density effluents being directly delivered to the slope. On the contrary, the fluvial facies point to braided streams with ordinary gravel and sand bars. The nontorrential character of the fluvial facies associated with the massive and simple (in opposition to complex) nature of the relatively thin gravity flow beds, which lack any internal erosional surface, are evocative of short-lived depletive surges instead of long-lived waxing to waning hyperpycnal currents (Mulder et al., 2003). A brief review of some criteria used elsewhere to recognize hyperpycnal flow deposits in the geological record and their correlation with the GF1 facies is presented in Table 1.

Although these two interpretations (sustained- versus surge-type) seem incompatible at first glance, the specific features that support each one are herein assembled in terms of an indirect fluvial control, that is, surgelike turbidity currents derived from the recurring failure of mouth-bar and delta-front sediments. It is also worth noticing that the clean nature of the sand- and gravel-rich GF1 strata, which display a very fine-grained (or coarser) sandy matrix, indicates that a large part of the fluvial suspended load (silt and clay) was not present in the turbidity currents.

Based on the concepts of Bates (1953) and Wright (1977), and on aforementioned pieces of evidence, it is assumed herein the existence of stratified fluvial effluents with well-defined bed and suspended load that did not enter the sea as inertia flows (truly hyperpycnal flows). Instead, friction-dominated fluvial effluents dumped their bed load (gravel and sand) in the delta front, whereas their suspended load was transported much farther as a hypopycnal plume. This case is similar, but not equal, to the subaerial inflow with an intermediate average density simulated by McLeod et al. (1999). This kind of inflow is strongly influenced by its internal stratification as its sediment-depleted upper layer (richer in finer grained suspended load) becomes a buoyant plume in the receiving basin, whereas its particulate-enriched lower section penetrates the tank as a dense flow. In the case presented herein, this lower sediment-enriched part of the flow could be responsible for the high rate of sediment fallout occurring in the delta front in conjunction with the tractive accumulation of the bed load.

Turbidity Currents Versus Sandy Debris Flows

Massive sandstones are dominant along the entire GF1 system. This fact stresses that other supporting mechanisms instead of fluid turbulence (e.g., fluid escape, hindered settling, and buoyancy) were important factors in the transport of the sediments, as in noncohesive sandy debris flows (Shanmugam, 2000). However, the quite distinct downcurrent grain-size segregation underlines the importance of the fluid turbulence in the long-distance transport of sand and gravel, that is, turbidity currents.

To accommodate such apparently conflicting ideas, bipartite turbidity currents, similar to the density-stratified flows envisaged by many authors (e.g., Kuenen, 1951; Bagnold, 1956; Sanders, 1965; Postma et al., 1988; Mutti et al., 1999), are proposed to equally explain the long (grain-size segregation caused by fluid turbulence)- and the short (ephemeral prefreezing basal inertia flows)-distance transport. The option for using the term "turbidity currents" instead of "noncohesive debris flows" emphasizes the long-distance mechanism of transport and its resultant facies tract instead of short-distance fluid rheology in the density flow basal layer and its associated massive fabric.

Autogenic and Allogenic Control

Autogenic and allogenic processes control the initiation of turbidity currents. As previously mentioned, turbidity current initiation has been related to high rates of sand and gravel deposition at distributary mouth bars during fluvial floods. This condition has induced the recurrent failure of the delta front and the resulting turbidity currents. However, as already presented, age (Gulisano and Gutierrez Pleimling, 1995) and sedimentologic (facies successions and associations) data about the shelf margin, slope, and basin-plain deposits indicate that GF1 surges were associated with high-frequency (4th to 5th order) lowstand stages and closely related short-lived shelf-margin deltas. This idea implies that an allogenic control, that is, relative sea level fall, is a major factor in promoting the right conditions for turbidity current triggering, that is, high rates of coarse-grained sediments (gravel and sand) being rapidly delivered over a relatively steep slope (lowstand shelf-margin deltas).

Table 1. **Positive (yes) and negative (no) correlation between features found in the GF1 deposit and some criteria used elsewhere in terms of hyperpycnal flow identification (from Paim et al., 2008).**

Criteria of Hyperpycnal Flow Recognition	*Reference*	*Correlation*
Physical connection between fluvial and turbidite channels at the shelf margin	Plink-Björklund and Steel (2004)	Yes, through small incised channels
Alternating massive and stratified intervals within a single bed	Plink-Björklund and Steel (2004); Bhattacharya and MacEachern (2008); Arcuri and Zavala (2008); Bourget et al. (2008); Vesely (2008)	No. Massive, stratified, or massive with stratified top discrete beds
Coarsening- and thickening-upward trend near the bed base and the reverse above		No. Thin, discrete, and uniform or graded beds
Abundant cut-and-fill features in a single bed		No. Absent
Laterally irregular grain-size changes		No. Absent
Sandy nature and abundant meter-scale beds	Piper and Savoye (1993); Mulder et al. (1998); Kneller and Buckee (2000); Mulder and Alexander (2001); Plink-Björklund and Steel (2004); Arcuri and Zavala (2008); Vesely (2008)	No. Gravel and sand as discrete decimeter-scale-thick beds
Systematically accreted shelf margin with associated turbidites	Plink-Björklund and Steel (2004)	Yes
Abundant continental plant material (leaves, phytodetritus, and coal fragments) in the turbidite beds	Mulder and Alexander (2001); Johnson et al. (2001); Plink-Björklund and Steel (2004)	Yes
Turbidite beds with lamination outlined by phytodetritus	Zavala (2008)	Yes, but more common in GF2 beds
Small amount of slump, slide, and debris-flow deposits	Plink-Björklund and Steel (2004)	No. High proportion of mass and debris-flow facies (GF3 facies)
Downcurrent pinch-out of thick beds of sandy turbidite	Plink-Björklund and Steel (2004)	No (only in GF2 strata)
Rounded and aligned mud clasts		Yes (usually aligned)
Siltstone and claystone-graded couplets with syneresis cracks	Bhattacharya and MacEachern (2008)	No, absent
Low to moderate trace fossil diversity, low bioturbation intensity, normal size ichnotaxa, lack of complex behavior strategies, suspension-feeding organisms	Bhattacharya and MacEachern (2008); Carmona et al. (2008)	Yes, usually low trace fossil diversity and bioturbation intensity and lack of complex behavior strategy

GF1 = first type of gravity flow system.

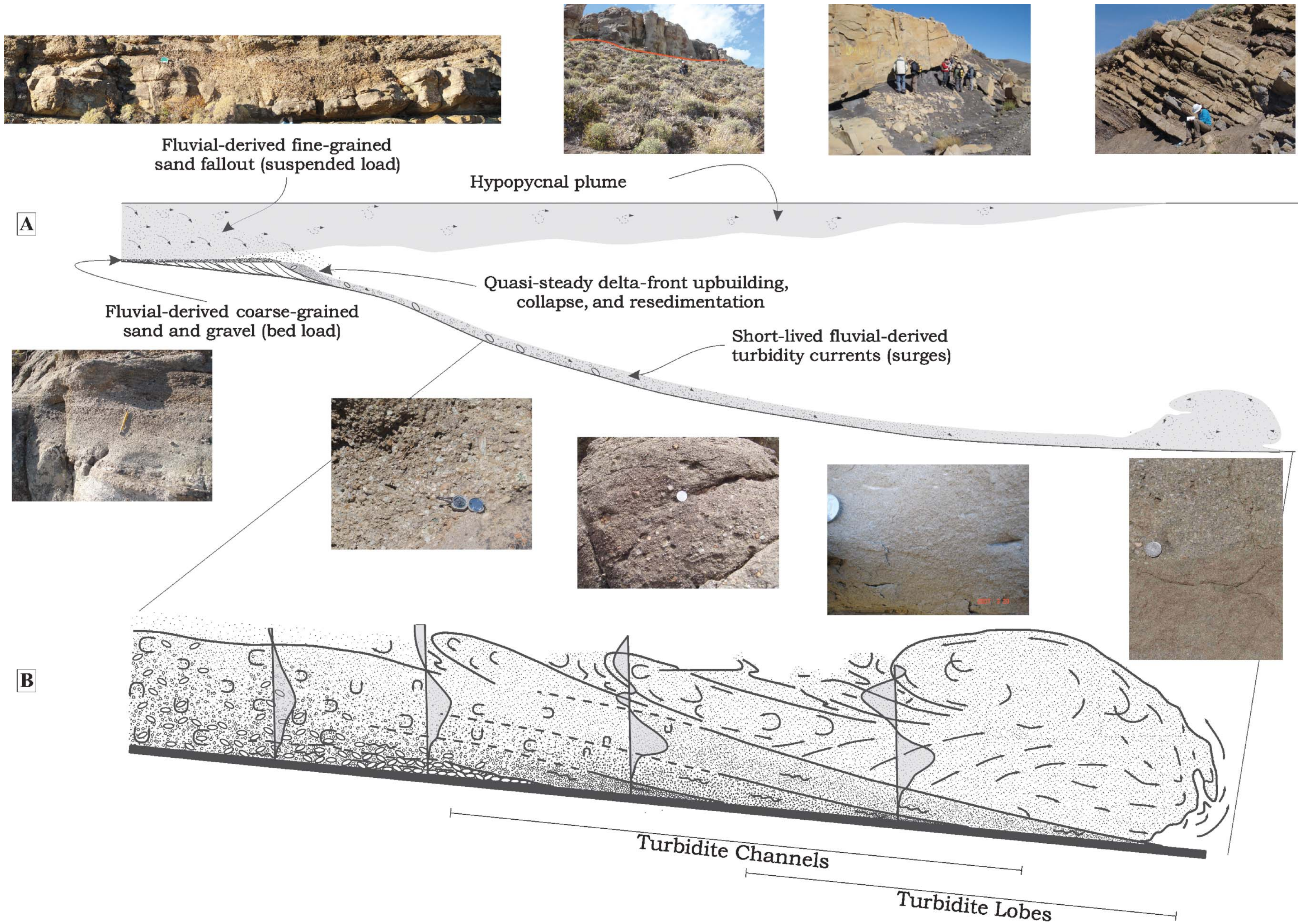

FIGURE 13. Conceptual model of triggering (A), transport with grain segregation (A, B) and deposition (B) of fluvial-derived turbidite surges. The top photographs exemplify the main architectural elements (incised fluvial channels, conglomeratic and sandy turbidite channels, and turbidite lobes), and photographs in the midportion represent the facies tract. Draft shown in panel B was adapted from Postma et al. (1988).

CONCLUDING REMARKS

Fluvial channels at the shelf margin, turbidite channels in the slope, and turbidite lobes and lobe fringes in the slope rise and basin plain represent the GF1 system in terms of architectural elements and physiographic settings. The increase of the gradient at the transition from the outer shelf to the slope enhances gravity flow buildup and entrenchment (turbidite channels in the slope), whereas the opposite alteration at the transition from the slope to the slope rise and basin plain favors large-scale sand deposition through poorly confined channels to widespread turbidite lobes. Multiple point sources related to high-frequency lowstand deltas gave origin to areas of high rates of sedimentation along the shelf margin.

The conceptual model (Figure 13) assumes average fluvial floods producing a quasi-steady delivery of sand and gravel onto continuously aggrading unstable delta-front ramps prograding into ever deeper water. Concurrently, the fluvial suspended load (silt and clay) was dispersed in the basin as hypopycnal plumes. After a brief storage period, debris flows were initiated through episodes of remobilization of the sediments deposited in the distributary mouth bars formed in such unstable areas. Because of flow acceleration along the slope, the gravity flow then builds up, becoming fully turbulent (turbidity current surges) and causing slope erosion. Subsequent deceleration produced a downcurrent grading through consecutive waves of sedimentation. These accumulation pulses were the result of gravity flow transformations driving flow bipartition and ensuing frictional freezing of the lower granular layers composed of ever finer grained sediments (massive strata). The lack of fine-grained particles in the turbidity currents, which results from flow separation at the mouth of the distributary channels, is indicated as the cause of the poor development of the truly tabular lobe beds and extensive lobe fringe facies as flow efficiency is likely to have diminished because of the small amount of clay in the fluid.

ACKNOWLEDGMENTS

This research was supported by Petróleo Brasileiro S. A. (Petrobras) and conducted within the terms of the Agreement for Cooperation and Technical Assistance signed by the Universidade do Vale do Rio dos Sinos (UNISINOS-Brazil) and the Secretaría de Estado de Energía y Minería de la Provincia del Neuquén (Argentina). Special thanks to M. Carminatti, J. E. Faccion, A. J. Andrade Ramos, O. C. Carbone (Petrobras), H. M. Palacios, C. E. Portilla, A. C. Garrido, J. C. Danieli, and Sergio Cocca (Secretaría de Estado de Energía y Minería de la Provincia del Neuquén).

REFERENCES CITED

Arcuri, M., and C. Zavala, 2008, Hyperpycnal shelfal lobes: Some examples from the Lotena and Lajas formations, Neuquén Basin, Argentina (abs.), *in* J. J. Ponce and E. B. Olivero, conveners, Sediment transfer from shelf to deepwater—Revisiting the delivery mechanisms: Conference Proceedings, AAPG Hedberg Research Conference, Ushuaia-Patagonia, Argentina, 4 p.

Bagnold, R. A., 1956, The flow of cohesionless grains in fluids: Philosophical Transactions of the Royal Society of London, Series A: Mathematical and Physical Sciences, v. 249, p. 235–297, doi:10.1098/rsta.1956.0020.

Bates, C. C., 1953, Rational theory of delta formation: AAPG Bulletin, v. 37, p. 2119–2162.

Bhattacharya, J. P., and J. A. MacEachern, 2008, Hyperpycnal rivers and prodeltaic shelves in the Cretaceous seaway of North America (abs.), *in* J. J. Ponce and E. B. Olivero, conveners, Sediment transfer from shelf to deepwater—Revisiting the delivery mechanisms: Conference Proceedings, AAPG Hedberg Research Conference, Ushuaia-Patagonia, Argentina, 4 p.

Bourget, J., S. Zaragosi, T. Mulder, T. Garlan, N. Ellouz-Zimmermann, A. Vantoer, and J.-L. Schneider, 2008, Monsoon-induced hyperpycnal flows recorded in the Gulf of Oman (NW Indian Ocean) (abs.), *in* J. J. Ponce and E. B. Olivero, conveners, Sediment transfer from shelf to deepwater—Revisiting the delivery mechanisms: Conference Proceedings, AAPG Hedberg Research Conference, Ushuaia-Patagonia, Argentina, 2 p.

Burguess, P. M., S. Flint, and S. Johnson, 2000, Sequence stratigraphic interpretation of the turbidítica strata: An example from Jurassic strata of the Neuquén Basin, Argentina: Geological Society of America Bulletin, v. 112, no. 11, p. 1650–1666, doi:10.1130/0016-7606(2000)112<1650:SSIOTS>2.0.CO;2.

Carmona, N., J. J. Ponce, M. I. Lopez-Cabrera, and E. Olivero, 2008, Trace fossil diversity in hyperpycnites: Ethologic implications and comparison to trace fossil in episodic gravity flows (abs.), *in* J. J. Ponce and E. B. Olivero, conveners, Sediment transfer from shelf to deepwater—Revisiting the delivery mechanisms: Conference Proceedings, AAPG Hedberg Research Conference, Ushuaia-Patagonia, Argentina, 2 p.

Fisher, R. V., 1983, Flow transformations in sediment gravity flows: Geology, v. 11, p. 273–274, doi:10.1130/0091-7613(1983)11<273:FTISGF>2.0.CO;2.

Gómez Omil, R. G., J. Schmithalter, A. Cangini, L. Albariño, and A. Corsi, 2002, El Grupo Cuyo en la Dorsal de Huincul: Consideraciones estratigráficas, tectónicas y petroleras, Cuenca Neuquina. Actas 5° Congreso de

Exploración y Desarrollo de Hidrocarburos, Mar del Plata Actas (CD-ROM).
Gradstein, F. M., J. G. Ogg, and A. G. Smith, 2004, A geologic time scale: Cambridge, Cambridge University Press, 589 p.
Gulisano, C. A., and A. R. Gutierrez Pleimling, 1995, Field guide: The Jurassic of the Neuquén Basin, Neuquén Province, Secretaria de Minería de la Nación (Publicación no. 158) y Asociación Geológica Argentina, Serie E (2), 111 p.
Helland-Hansen, W., and J. G. Gjelberg, 1994, Conceptual basis and variability in sequence stratigraphy: A different perspective: Sedimentary Geology, v. 92, p. 31–52, doi:10.1016/0037-0738(94)90053-1.
Heller, P. L., and W. R. Dickinson, 1985, Submarine ramp facies model for delta-fed, sand-rich turbidite systems: AAPG Bulletin, v. 69, no. 6, p. 960–976.
Hunt, D., and M. E. Tucker, 1992, Stranded parasequences and the forced regressive wedge systems tract: Deposition during base-level fall: Sedimentary Geology, v. 81, p. 1–9, doi:10.1016/0037-0738(92)90052-S.
Johnson, K., C. K. Paull, J. P. Barry, and F. P. Chavez, 2001, A decal record of underflows from a coastal river into the deep sea: Geology, v. 29, p. 1019–1022, doi:10.1130/0091-7613(2001)029<1019:ADROUF>2.0.CO;2.
Kneller, B., and C. Buckee, 2000, The structure and fluid mechanics of turbidity currents: A review of some recent studies and their geological implications: Sedimentology, v. 47, no. 1, p. 62–94, doi:10.1046/j.1365-3091.2000.047s1062.x.
Kochhann, K. G. D., S. Baecker-Fauth, G. Fauth, A. S. Silveira, 2009, Aalenian (middle Jurassic) radiolarian fauna from Los Molles Formation, Argentina, and its paleobiogeographic affinities, *in* Congresso Brasileiro de Paleontologia, 2009, Livro de Resumos, v. 1, p. 39.
Kuenen, Ph. H., 1951, Properties of turbidity currents of high density, *in* J. L. Hough, ed., Turbidity currents and the transportation of coarse sediments to deepwater: A symposium: SEPM Special Publication 2, p. 14–33.
Leanza, H. A., and C. A. Hugo, 1997, Hoja Geológica 3969-III, Picún Leufú, provincias del Neuquén y Río Negro, Programa Nacional de Cartas Geológicas de la República Argentina, escala 1: 250.000: Boletín Instituto de Geología y Recursos Naturales, v. 218, p. 1–135.
Legarreta, L., and C. A. Gulisano, 1989, Análisis estratigráfico secuencial de la Cuenca Neuquina (Triásico superior-Terciario inferior, Argentina), *in* G. Chebli and L. Spalletti, eds., Cuencas sedimentarias Argentinas, Instituto Miguel Lillo, Universidad Nacional de Tucumán, San Miguel de Tucumán, Serie Correlación Geológica 6, p. 221–243.
Legarreta, L., and M. A. Uliana, 1991, Jurassic/Cretaceous marine oscillations and geometry of a back-arc basin fill, central Argentine Andes, *in* D. I. M. Mc Donald, ed., Sedimentation, tectonics and eustasy: Oxford, International Association of Sedimentologists Special Publication 12, p. 429–450.
McLeod, P., S. Carey, and R. S. J. Sparks, 1999, Behavior of particle-laden flows into the ocean: Experimental simulation and geological implications: Sedimentology, v. 46, p. 523–536, doi:10.1046/j.1365-3091.1999.00229.x.
Mulder, T., and J. Alexander, 2001, The physical character of subaqueous sedimentary density flows and their deposits: Sedimentology, v. 48, p. 269–299, doi:10.1046/j.1365-3091.2001.00360.x.
Mulder, T., J. P. M. Syvitski, and K. I. Skene, 1998, Modeling of erosion and deposition of turbidity currents generated at river mouths: Journal of Sedimentary Research, v. 68, p. 124–137.
Mulder, T., J. P. M. Syvitski, S. Nigeon, J. C. Faugeres, and B. Savoye, 2003, Marine hyperpycnal flows: Initiation, behavior and related deposits—A review: Marine and Petroleum Geology, v. 20, p. 861–882, doi:10.1016/j.marpetgeo.2003.01.003.
Mutti, E., 1992, Turbidite sandstones San Donato Milanese: Parma, Italy, Azienda Generale Italiana Petroli-Instituto di Geologia, Università di Parma, p. 275.
Mutti, E., R. Tinterri, E. Remacha, N. Mavilla, S. Angela, and L. Fava, 1999, An introduction to the analysis of ancient turbidite basins from an outcrop perspective, AAPG Continuing Education Course Note Series 39, p. 61.
Mutti, E., R. Tinterri, G. Benevelli, D. Di Biase, and G. Cavanna, 2003, Detaic, mixed and turbidite sedimentation of ancient foreland basins: Marine and Petroleum Geology, v. 20, p. 733–755, doi:10.1016/j.marpetgeo.2003.09.001.
Paim, P. S. G., A. S. Silveira, E. L. C. Lavina, U. F. Faccini, H. A. Leanza, J. M. M. Teixeira de Oliveira, and R. S. F. d'Ávila, 2008, High resolution stratigraphy and gravity flow deposits in the Los Molles Formation (Cuyo Group-Jurassic) at La Jardinera region, Neuquén Basin, Argentina: Revista de la Asociación Geológica Argentina, v. 63, no. 4, p. 728–753.
Pierson, T. C., and J. E. Costa, 1987, A rheologic classification of subaerial sediment-water flows, *in* J. E. Costa and G. F. Wieczorek, eds., Debris flows/avalanches: Process, recognition, and mitigation: Geological Society of America Reviews in Engineering Geology, v. VII, p. 1–12.
Piper, D. J. W., and B. Savoye, 1993, Processes of Late Quaternary turbidity current flow and deposition on the Var fan, north-west Mediterranean Sea: Sedimentology, v. 40, p. 557–582, doi:10.1111/j.1365-3091.1993.tb01350.x.
Plink-Björklund, P., and R. J. Steel, 2004, Initiation of turbidity currents: Outcrop evidence for Eocene hyperpycnal flow turbidites: Sedimentary Geology, v. 165, p. 29–52, doi:10.1016/j.sedgeo.2003.10.013.
Postma, G., W. Nemec, and K. L. Kleinspehn, 1988, Large floating clasts in turbidites: A mechanism for their emplacement: Sedimentary Geology, v. 58, p. 47–61, doi:10.1016/0037-0738(88)90005-X.
Ramos, V. A., 1998, Estructura del sector occidental de la Faja Plegada y Corrida del Agrio, Cuenca Neuquina, Argentina, Actas 10° Congreso Latinoamericano Geología y 6° Congreso Nacional Geología Económica 2, Buenos Aires, Argentina, p. 105–110.

Sanders, J. E., 1965, Primary sedimentary structures formed by turbidity currents and related sedimentation mechanisms, *in* G. V. Middleton, ed., Primary sedimentary structures and their hydrodynamic interpretations: SEPM Special Publication 12, p. 192–219.

Shanmugam, G., 2000, 50 Years of the turbidite paradigm (1950s–1990s): Deep-water processes and facies models—A critical perspective: Marine and Petroleum Geology, v. 17, p. 285–342, doi:10.1016/S0264-8172(99)00011-2.

Steel, R. J., J. Crabaugh, M. Schellpeper, D. Mellere, P. Plink-Björklund, J. Deibert, and T. Loeseth, 2000, Deltas vs. river on the shelf edge: Their relative contributions to the growth of the shelf-margin and basin-floor fans (Barreminan to Eocene, Spitsbergen), *in* P. Weimer, ed., Deep-water reservoirs of the world: Gulf Coast Section-Society of Sedimentary Geology (GC-SEPM) Research Conference (CD-ROM), p. 981–1009.

Van Wagoner, J. C., H. W. Posamentier, R. M. Mitchum Jr., P. R. Vail, J. F. Sarg, T. S. Loutit, and J. Hardenbol, 1988, An overview of the fundamentals of sequence stratigraphy and key definitions, *in* C. K. Wilgus, B. S. Hastings, C. G. St. C. Kendall, H. W. Posamentier, C. A. Ross, and J. C. Van Wagoner, eds., Sea level changes: An integrated approach: SEPM Special Publication 42, p. 40–45.

Van Wagoner, J. C., R. M. Mitchum Jr., K. M. Campion, and V. D. Rahmanian, 1990, Siliciclastic sequence stratigraphy in well logs, cores, and outcrops: Concepts for high-resolution correlation of time and facies: AAPG Methods in Exploration Series 50, 10, p. 2150–2175.

Vergani, G. D., 2005, Control estructural de la sedimentación jurásica (Grupo Cuyo) en la Dorsal de Huincul, Cuenca Neuquina, Argentina, Modelo de falla lístrica rampa-plano, invertida: Boletín de Informaciones Petroleras, v. 1, no. 1, p. 32–42.

Vergani, G. D., A. J. Tankard, H. J. Belotti, and H. J. Welsink, 1995, Tectonic evolution and paleogeography of the Neuquén Basin, Argentina, *in* A. J. Tankard, R. Suárez Soruco, and H. J. Welsink, eds., Memoir petroleum basins of South America: AAPG Bulletin, v. 62, p. 383–402.

Verzi, H., M. F. Raggio, and M. Suarez, 2005, Volume interpretation of a turbidite system, Los Molles Formation, Neuquén Basin, Argentina, *in* D. Soubies, M. Arteaga, and F. Fantín, eds., La Sísmica de Reflexión, más allá de la Imagen Estructural, Buenos Aires, Instituto Argentino del Petroleo y del Gas, 2005, p. 219–226.

Vesely, F. F., 2008, Subaqueous sandstones deposited by melt water-fed density flows in a late Paleozoic glaciomarine succession, eastern Paraná Basin, Brazil (abs.), *in* J. J. Ponce and E. B. Olivero, conveners, Sediment transfer from shelf to deepwater—Revisiting the delivery mechanisms: Conference Proceedings, AAPG Hedberg Research Conference, Ushuaia-Patagonia, Argentina, 1 p.

Vicente, J. C., 2005, Dynamic paleogeography of the Jurassic Andean Basin: Pattern of regression and general considerations of the main features: Revista de la Asociación Geológica Argentina, v. 61, no. 3, p. 408–437.

Wright, L. D., 1977, Sediment transport and deposition at river mouths: A synthesis: Geological Society of America Bulletin, v. 88, p. 857–868, doi:10.1130/0016-7606(1977)88<857:STADAR>2.0.CO;2.

Zavala, C., 1993, Estratigrafía y análisis de facies de la Formación Lajas (Jurásico medio) en el sector sur occidental de la Cuenca Neuquina. Provincia del Neuquén, República Argentina, Tesis Doctoral Departamento de Geología, Universidad Nacional del Sur, Bahía Blanca, Buenos Aires, Argentina, 260 p.

Zavala, C., 2008, Toward a genetic facies tract for the analysis of hyperpycnal deposits (abs.), *in* J. J. Ponce and E. B. Olivero, conveners, Sediment transfer from shelf to deepwater—Revisiting the delivery mechanisms: Conference Proceedings, AAPG Hedberg Research Conference, Ushuaia-Patagonia, Argentina, 3 p.